

## Analysis of the Spatio-temporal Patterns of Wildfire Susceptibility in Queen Elizabeth National Park (QENP) – Uganda

Derrick Robert Irumba<sup>1</sup>, Anthony Gidudu (PhD)<sup>2</sup>, Lydia Mazzi Kayondo (PhD)<sup>3</sup>

<sup>1</sup> Department of Geomatics and Land Management, College of Engineering, Design, Art Technology, Makerere University, P.O. Box 7062, Kampala, Uganda, [drirumba@gmail.com](mailto:drirumba@gmail.com)

<sup>2</sup> Department of Geomatics and Land Management, College of Engineering, Design, Art Technology, Makerere University, P.O. Box 7062, Kampala, [anthony.gidudu@gmail.com](mailto:anthony.gidudu@gmail.com)

<sup>3</sup> Department of Geomatics and Land Management, College of Engineering, Design, Art Technology, Makerere University, P.O. Box 7062, Kampala, Uganda, [ldandiko@gmail.com](mailto:ldandiko@gmail.com)

DOI: <https://dx.doi.org/10.4314/sajg.v14i1.4>

### Abstract

*This study determined the variability of wildfire susceptibility in Queen Elizabeth National Park (QENP) in space and time. QENP is a protected area in Western Uganda. MODIS and VIIRS data for a six-and-a-half-year period from January 2015 - June 2021 were obtained to create an inventory of past fires. From these fires, spatial and temporal patterns were derived from exploratory spatial data analyses. The Weights of Evidence (WOE) method, a Bayesian form of statistical modelling, was used to determine the relationship between fires and wildfire conditioning factors, as well as to model wildfire susceptibility. Results of the study showed that the occurrence of wildfires within the study area vary seasonally. Sixty-one percent (61%) of the fires were observed to occur in the first dry season of the year, while thirty-one percent (31%) of the fires were observed to occur in the second dry season. Among the wildfire conditioning factors, altitude, vegetation (as measured by NDVI), and proximity to lakes indicated the highest correlation with the occurrence of fires. These conditions were attributed to physiographic influences, water stress in vegetation, and the socio-economic activities of the fishing villages around the lakes respectively. From the derived wildfire susceptibility maps, varying levels of wildfire susceptibility were determined. Proportional values of 19% and 20% of the study area were classified with very high and high susceptibility levels respectively. The remaining 61% of the study area was covered by moderate, low, and very low susceptibility levels. The study results provided vital findings about the seasonal patterns of wildfire occurrence, factors influencing the occurrence of wildfires and the locations most susceptible to wildfires. This information will enable managers to allocate fire management resources optimally to efficiently mitigate against wildfires within QENP.*

**Keywords:** Wildfires, Wildfire Susceptibility, Weights of Evidence, QENP

### 1. Introduction

Wildfires are considered as one of the major threats to vegetated areas (Sánchez *et al.*, 2018). They are a common phenomenon in most of the vegetated landscapes in Sub-Saharan Africa (SSA) (Wimberly *et al.*, 2024). This is attributed to the existence of vast savannah grasslands that support burning, as well as a fire-conducive climate that comprises a chronic rhythm of wetting and drying that allows for the

growth of vegetation in the wet season and its withering in the dry season, thus preparing it for burning. The savannahs and forests of West African countries, the East and Central African grasslands, and the fynbos biomes of the Cape region in Southern Africa are some of the notable parts of the SSA region that frequently experience wildfires (Global Fire Monitoring Center, 2004). In these regions, Protected Areas (PAs) such as national parks are some of the landscapes that have been increasingly affected by wildfires (Nhongo *et al.*, 2019; Plumptre *et al.*, 2010).

Wildfires impact both wildlife and vegetation, leading, amongst their other effects, to animal deaths and loss of biodiversity (Jaafari *et al.*, 2019; Jones *et al.*, 2022; Xue *et al.*, 2024). To counteract the adverse effects of wildfires, authorities in PAs are required to effectively implement fire management in the form of prevention and suppression practices, with much emphasis on the former (Adab *et al.*, 2015). Fire prevention involves proactive practices that are applied before wildfires occur, while fire suppression involves reactive measures aimed at extinguishing active wildfires. However, for the effective application of fire prevention and suppression mechanisms to be carried out, knowledge regarding fire behavior and to identify fire-prone areas is necessary (Food and Agriculture Organisation of the United Nations, 2006). Unfortunately, PAs in SSA often lack updated information, not only concerning the behavior and pattern of fires, but also the areas susceptible to wildfires (DeMeo *et al.*, 2010).

The availability of detailed, reliable maps and periodic updates of them can provide vital information to facilitate effective wildfire management (Sánchez *et al.*, 2018). This can be accomplished through the application of the remotely sensed satellite products currently available (Global Fire Monitoring Center, 2004). These can be used to study the pattern and behavior of fires, as well as to identify fire-prone areas in various landscapes through wildfire susceptibility modelling. Thus, wildfire susceptibility modelling becomes a vital tool for landscape managers in the identification of locations posing high wildfire risks and leading to the optimization and allocation of resources for fire management (Nhongo *et al.*, 2019).

Wildfire susceptibility modelling typically starts with the identification and creation of a database containing records of past fire events (Jaafari *et al.*, 2019; Xue *et al.*, 2024). The documenting of historical fire events can be carried out by using a variety of data sources, such as satellite imagery, aerial photography, observations made and records taken during fieldwork, and historical archives (Jaafari *et al.*, 2017). However, satellite data is more advantageous as it presents opportunities for global coverage on different spatial and temporal scales (Verbesselt *et al.*, 2006; Xue *et al.*, 2024). Active fire datasets that can be used in the documentation of past fire events can be obtained from the Moderate Resolution Imaging Spectroradiometer (MODIS) hotspot product and the Visible Infrared Imaging Radiometer Suite (VIIRS). The daily and global availability of MODIS and VIIRS fire data makes them most suitable for application in fire studies (Molaudzi & Adelabu, 2018).

Upon documentation of historical fire events, there is a need to ascertain the wildfire conditioning factors and identify the prospective relationships between the conditioning factors and past fires (Jaafari

*et al.*, 2019). Determination of potential relationships between influential factors and historical fires can be achieved by employing either knowledge-based or data-based models. Data-based models are preferred as knowledge-based models are subjective owing to their reliance on expert opinion (Adab *et al.*, 2015). Examples of methods with the widest application in wildfire susceptibility modelling include logistic regression (Chuvieco & Congalton, 1989; Pourghasemi, 2015), Analytical Hierarchy Process (AHP) (Jaafari *et al.*, 2019; Kayijamahe *et al.*, 2020), the use of Frequency Ratio (FR) (Pourtaghi *et al.*, 2016), the application of the Weights of Evidence (WOE) method (Hong *et al.*, 2019; Jaafari *et al.*, 2017), Evidential Belief Function (EBF) (Nami *et al.*, 2018), and the Random Forest (RF) method (Ghorbanzadeh *et al.*, 2019).

The main objective of this study was to determine the spatio-temporal variability of wildfire susceptibility in the case of Queen Elizabeth National Park (QENP) in Uganda using MODIS and VIIRS active fire data. This was accomplished by characterizing the relationship between wildfire conditioning factors and fires in a spatio-temporal perspective by using the WOE method, as well as by modelling wildfire susceptibility. The study was aimed at providing vital information regarding the behaviour and pattern of wildfires and at identifying the fire-prone areas within QENP for the effective management of wildfires.

## **2. Study Area**

The study was carried out in the QENP, a PA located in Western Uganda (Figure 1).

QENP covers 1,978 km<sup>2</sup> and is crossed by the equator in the Albertine Rift Valley (Uganda Wildlife Authority, 2012a). It lies between 0° 15'N and 0° 45'S latitude and 29° 35'E and 30° 20'E longitude. Like all national parks and wildlife reserves in Uganda, QENP is managed by the Uganda Wildlife Authority (UWA). The park is uniquely divided into northern and southern sections by the Kazinga channel, a waterway that connects Lake Edward on the western end of the park and Lake George on the eastern end. QENP is part of a much larger transboundary grassland-forest-wetland ecosystem (CARE-Uganda, 2007). QENP comprises of two major vegetation types and lies at their convergence. These are the Central African rainforest and the East African grasslands, both consisting of diverse habitats, including open grasslands, thickets, thick bush, forests, wetlands, and a lakeshore of 250 Km (UWA, 2012b).

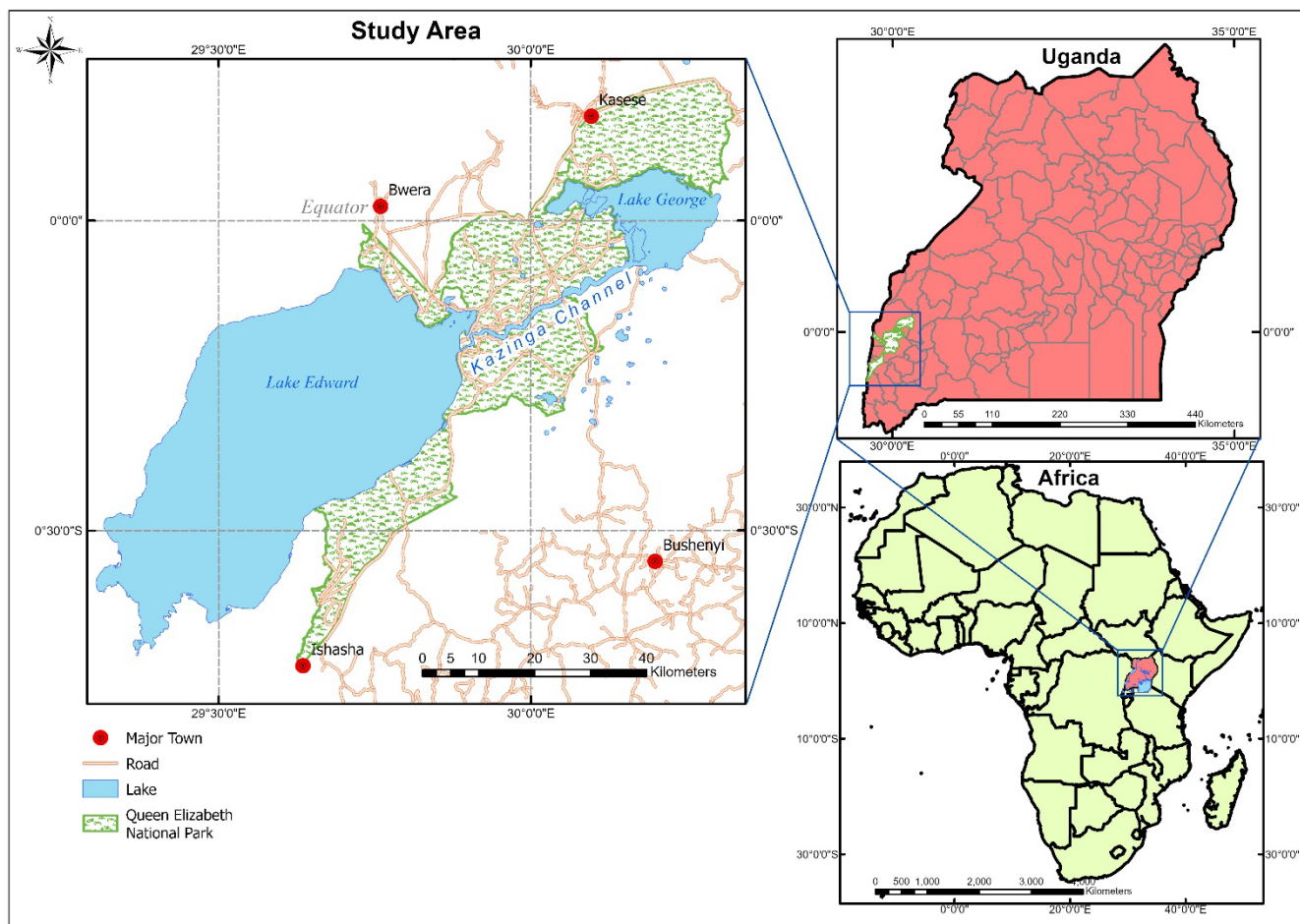


Figure 1: Location of Study Area

### 3. Data and Methods

#### 3.1. Data and Wildfire Conditioning Factors

##### 3.1.1. Inventory of Past Wildfire Events

MODIS hotspot and VIIRS active fire products were used to compile the inventory of fire events. Both products were used in the study to not only ascertain and exploit their merits, but also provide the basis for a comparison. The fire events served as the dependent (exploratory) variable for the wildfire susceptibility modelling. Since most fires in the study area are human induced, with the majority unintentional (UWA, 2012), it was assumed that all the fires under investigation were wildfires. The MODIS hotspot and VIIRS active fire products were obtained from the FIRMS Portal (<http://earthdata.nasa.gov/firms>) as points in shapefile format. The fire datasets were downloaded for the period, January 2015 - June 2021. A study period of six-and-a-half-years was selected because it allowed for the acquisition of a substantial number of fire events to establish meaningful statistical relationships with fire conditioning factors.

### *3.1.2. Wildfire Conditioning Factors*

The wildfire conditioning factors served as independent (explanatory) variables for the susceptibility modelling. From the various studies, however, there is no clear agreement on which wildfire conditioning factors are the most useful for modelling wildfire susceptibility (Hong *et al.*, 2019). Different studies employ conditioning factors based on the landscapes they study. Based on studies (Adab *et al.*, 2015; Ghorbanzadeh *et al.*, 2019; Hong *et al.*, 2019; Jahdi *et al.*, 2016; Kayijamahe *et al.*, 2020; Kganyago & Shikwambana, 2019), the availability of data and the nature of the study area, potential wildfire conditioning factors included the topographic factors of altitude and aspect; precipitation; vegetation (as measured by the Normalized Difference Vegetation Index (NDVI)); and proximity to roads, waterbodies, and settlements.

Altitude and aspect were derived from a Digital Elevation Model (DEM) generated from Advanced Space-borne Thermal Emission and Reflection Radiometer (ASTER) data. The 30m resolution ASTER data were obtained from the USGS geoportal (<https://earthexplorer.usgs.gov/>). Precipitation data for the years 2015-2019 were obtained from the Climate Hazards Group InfraRed Precipitation with Station data (CHIRPS) portal (<https://www.chc.ucsb.edu/data/chirps>). NDVI was derived from 30m resolution Landsat data. The cloud-free Landsat Enhanced Thematic Mapper (ETM+) (Landsat 7) and the Operational Land Imager (OLI)-Landsat 8 data were obtained from the USGS geoportal. The study area was covered by images in two scenes and therefore two images were downloaded for each year. Vector datasets for roads, waterbodies (lakes and rivers), and settlements (villages) were obtained from an existing database at the Uganda Bureau of Statistics (UBOS). The vector datasets were used to derive proximity factors.

The ASTER DEM was subset to extract data for the study area DEM. From this, altitude data were extracted, after which slope, and aspect were computed. The precipitation data were in grid format at 0.05° resolution, with each image providing average annual precipitation values. The grid data were then projected to WGS 1984 UTM zone 36 N and subset to extract the study area precipitation raster. The subset images were then resampled to 30 m to match the resolution of the other variables. The yearly resampled precipitation images were averaged to obtain the mean precipitation values of the study area over the study period. Preprocessing of the Landsat images was carried out and this included gap filling (for Landsat 7), radiometric calibration, atmospheric correction, layer stacking, mosaicking, and image registration. The NDVI was computed from the geometrically corrected images for each year of the study. The resultant NDVI images for each year were then subset to extract the values for the study area. The yearly images were then averaged to obtain the mean NDVI values of the study area over the study period. To determine proximity to roads, lakes, rivers, and settlements, Euclidian distance computations were carried out to generate raster datasets with a grid size of 30 m. The raster datasets were then subset

according to the study area. All wildfire conditioning factors were processed as continuous variables. The continuous datasets were then categorized with ranges of values suited to the study area.

### **3.2. Methods**

#### *3.2.1. Spatio-temporal Analysis of Fire Data*

Based on the locations of fire events, queries were then carried out to determine any patterns in their spatial distribution. Fire dataset attributes, such as the date of collection, were then used in temporal analyses by building attribute-based queries. Exploratory spatial data analyses were then carried out on the results of the queries, thereby leading to the creation of histograms to represent monthly and annual distributions of fire events. Temporal patterns and trends were then derived from the histograms.

#### *3.2.2. Assessment of Multi-collinearity*

For applications of the WOE model, the explanatory variables should not exhibit multi-collinearity. Multi-collinearity exists when two or more explanatory variables are strongly correlated. To ensure that the explanatory variables considered are not correlated, a multi-collinearity diagnostic was carried out. Determination of Variance Inflation Factors (VIF), which is the most common method to check for multi-collinearity among explanatory variables (Jaafari *et al.*, 2017), was applied. Variables with values of VIF >5 exhibit multi-collinearity (Jaafari *et al.*, 2018).

#### *3.2.3. Determining the Relationship between Wildfire Events and Wildfire Conditioning Factors using the WOE Method*

The WOE method was used to determine the relationship between fire events and the fire conditioning factors by calculating a set of weights, with one weight for each factor category, as elucidated by Lee *et al.* (2012). The WOE method was selected because it uses a straightforward analytic framework (Jaafari *et al.*, 2019).

The weight for a given wildfire conditioning factor (T) was computed based on the presence or absence of a wildfire event (F) (Lee *et al.*, 2012). A positive weight ( $W^+$ ) indicated the presence of a causative factor for a wildfire, and the magnitude of this weight was an indication of the positive correlation between the presence of a causative factor and a wildfire event (Ozdemir & Altural, 2013). The positive weight was computed using Equation [1]. A negative weight ( $W^-$ ) indicated an absence of a causative factor for a wildfire, and the magnitude indicated a negative correlation between the presence of a causative factor and a wildfire event (Ozdemir & Altural, 2013). The negative weight was computed using Equation [2].

$$W^+ = \log_e \left\{ \frac{P(T|F)}{P(T|\bar{F})} \right\} \tag{1}$$

$$W^- = \log_e \left( \frac{P(\bar{T}|F)}{P(\bar{T}|\bar{F})} \right) \quad [2]$$

The difference in weights, also known as the weights contrast (C), was then computed to reflect the overall association between the conditioning factor category and the wildfire event. C was computed using Equation [3]. A contrast value equal to zero indicated that the considered class of conditioning factors was not significant to the analysis. A positive contrast indicated a positive spatial correlation, and the opposite (*vice versa*) for a negative contrast (Lee *et al.*, 2012). The final weight ( $W_{\text{final}}$ ), also known as the studentized value of C for a given class of conditioning factor, was then calculated using Equation [4]. For a given conditioning factor, the higher the value of  $W_{\text{final}}$ , the higher the significance of the category, and *vice versa* (Jaafari *et al.*, 2017). The associations and levels of significance between wildfire conditioning factors and wildfire locations were then derived from C and  $W_{\text{final}}$  respectively.

$$C = W^+ - W^- \quad [3]$$

$$W_{\text{final}} = C/S(C) \quad [4]$$

$$S(C) = \sqrt{S^2(W^+) + S^2(W^-)} \quad [5]$$

Where S(C) is the standard deviation of the contrast given by Equation [5].

#### 3.2.4. Modelling Wildfire Susceptibility and Validation

$W_{\text{final}}$  was used to produce multi-category weighted factors for all explanatory variables. This was done by assigning the values of  $W_{\text{final}}$  to the corresponding explanatory variable category. To obtain the first model, the multi-category weighted explanatory variables were overlaid and numerically added to produce fire susceptibility index maps.

The Receiver Operating Characteristic (ROC) Area Under the Curve method, known as the ROC-AUC method, was used to validate the model results. The method was selected because it is commonly used for characterizing the quality of susceptibility approaches (Ghorbanzadeh *et al.*, 2019; Hong *et al.*, 2018). A ROC curve plots changes in true positive prediction rates *versus* false positive prediction rates and starts at the points (0,0) and reaches (1,1) (Jaafari *et al.*, 2017). The highest possible area under the curve, where AUC =1, represents the classification in which all fire pixels and all non-fire pixels are correctly predicted. AUC values of <0.6 signify a poor, 0.6–0.7 a moderate, 0.7–0.8 a good, 0.8–0.9 a very good, and >0.9 an excellent model performance (Gralewicz *et al.*, 2011). Validation was carried out on all susceptibility index maps using the ROC-AUC method to obtain the most optimally performing model.

To evaluate the impact of each explanatory variable on wildfire susceptibility and assess uncertainties, the process was repeated, omitting one variable at a time. At every iteration, a new model was created,

and a susceptibility index map generated. For each developed model, validation was carried out by computing the ROC-AUC to check its performance. The model with the best performance was then used to produce the final susceptibility map for MODIS and the VIIRS-derived WOE data.

## **4. Results and Discussion**

### **4.1. Location and Distribution of Fires**

A total of 534 and 1,585 fire events were obtained from the MODIS and VIIRS datasets respectively. For the MODIS data, 374 fire events (70% of the total) were randomly obtained to be used for model training, and 160 fire events (30% of the total) for model validation. Similarly, for the VIIRS data, 1,110 fire events (70% of the total) were randomly obtained to be used for model training and 475 fire events (30% of the total) for model validation. VIIRS data comprised three times more fire events than the MODIS data. The higher number of fires is due to an improvement in the fire detection rate achieved by the VIIRS instrument. The increased fire detection rate is because of the higher spatial resolution (375m) of the VIIRS, and the unique sampling scheme as compared to the one-kilometer spatial resolution of the MODIS model (Schroeder *et al.*, 2014).

As previously discussed, the study area is divided into northern and southern sections by the Kazinga channel waterway; 317 MODIS fire locations (60% of the total) and 916 VIIRS fire locations (58% of the total) were observed in the northern section, while 217 MODIS fire locations (40% of the total) and 669 VIIRS fire locations (42%) were observed in the southern section (Figure 2). Most fire locations were observed in the northern section of the park. This concurs with the findings of previous studies by Jaksic-Born (2009) and observations by Uganda Wildlife Authority (2012). Areas north of the Kazinga channel generally experience frequent fires owing to the grassland expanses which are much larger than those of the southern areas (Uganda Wildlife Authority, 2012a).

For the duration of the study period, fires observed in the study area presented with two peak seasons, namely, January - March (with January experiencing the most fires) and June - August (with July experiencing the most fires) in accordance with previous studies (Jaksic-Born, 2009; Plumptre *et al.*, 2010) (Figure 3). The January - March season was observed to experience the greater number of fires as compared to the June - August season. From the MODIS data, the January - March season experienced 326 fires (approximately 61% of the total) and the June - August season experienced 168 fires (approximately 31 % of the total). From the VIIRS data, the January - March season experienced 941 fires (approximately 60% of the total) and the June - August season experienced 496 fires (approximately 31 % of the total). It should be noted that these two peak fire seasons coincide with the two dry seasons that the study area experiences. These dry seasons are characterized by high temperatures that aid in the drying out of the vegetation, hence providing conducive conditions for it in which to burn. The dry



seasons also coincide with the periods in which farmers in communities within the park prepare their lands for cultivation in the subsequent wet season. These preparations involve the burning of dried stalks and vegetation in a bid to clear their lands for plowing. Fires related to these burning practices can easily spread into the park, thereby resulting in wildfires.

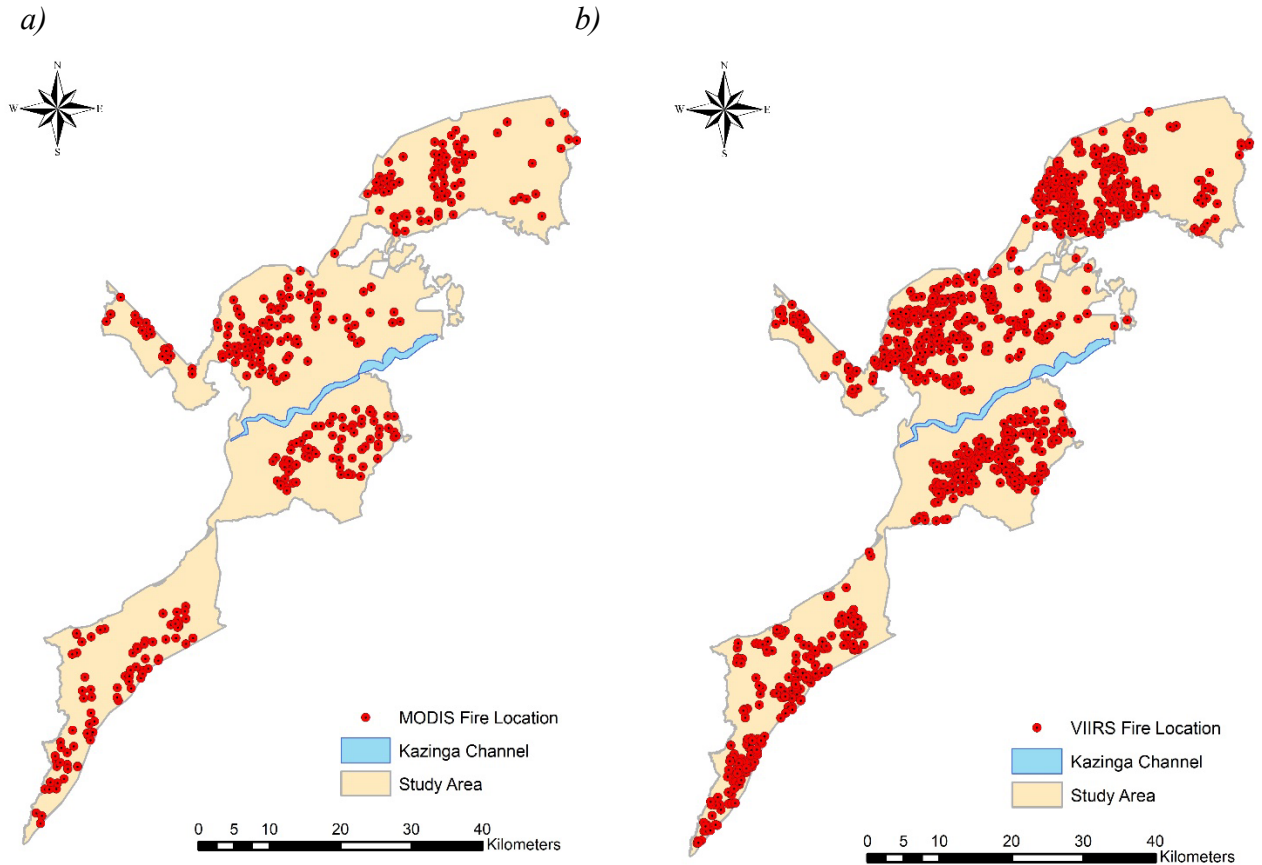


Figure 2: Fire Distribution: a) MODIS model; b) VIIRS model

#### 4.2. Wildfire Conditioning Factors

The wildfire conditioning factors are shown in Figure 4. Water bodies were split further into lakes and rivers to derive distance from lakes and distance from rivers, each variable considered as an independent wildfire conditioning factor.

#### 4.3. Assessment of multi-collinearity

Variance Inflation Factor (VIF) values derived using both MODIS and VIIRS data indicated that all factors were below the critical value of five (5) and therefore none of the factor was correlated. Therefore, following these results, all variables were retained for modelling.

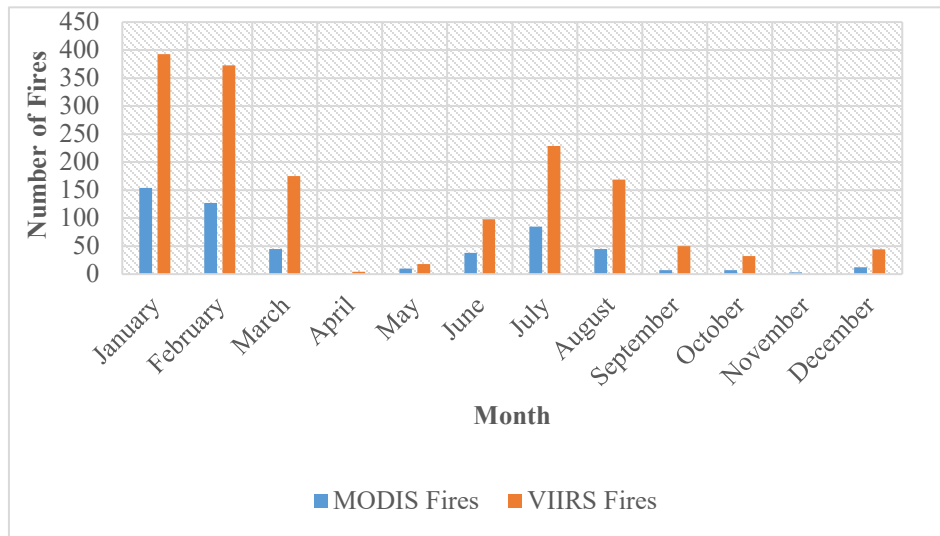
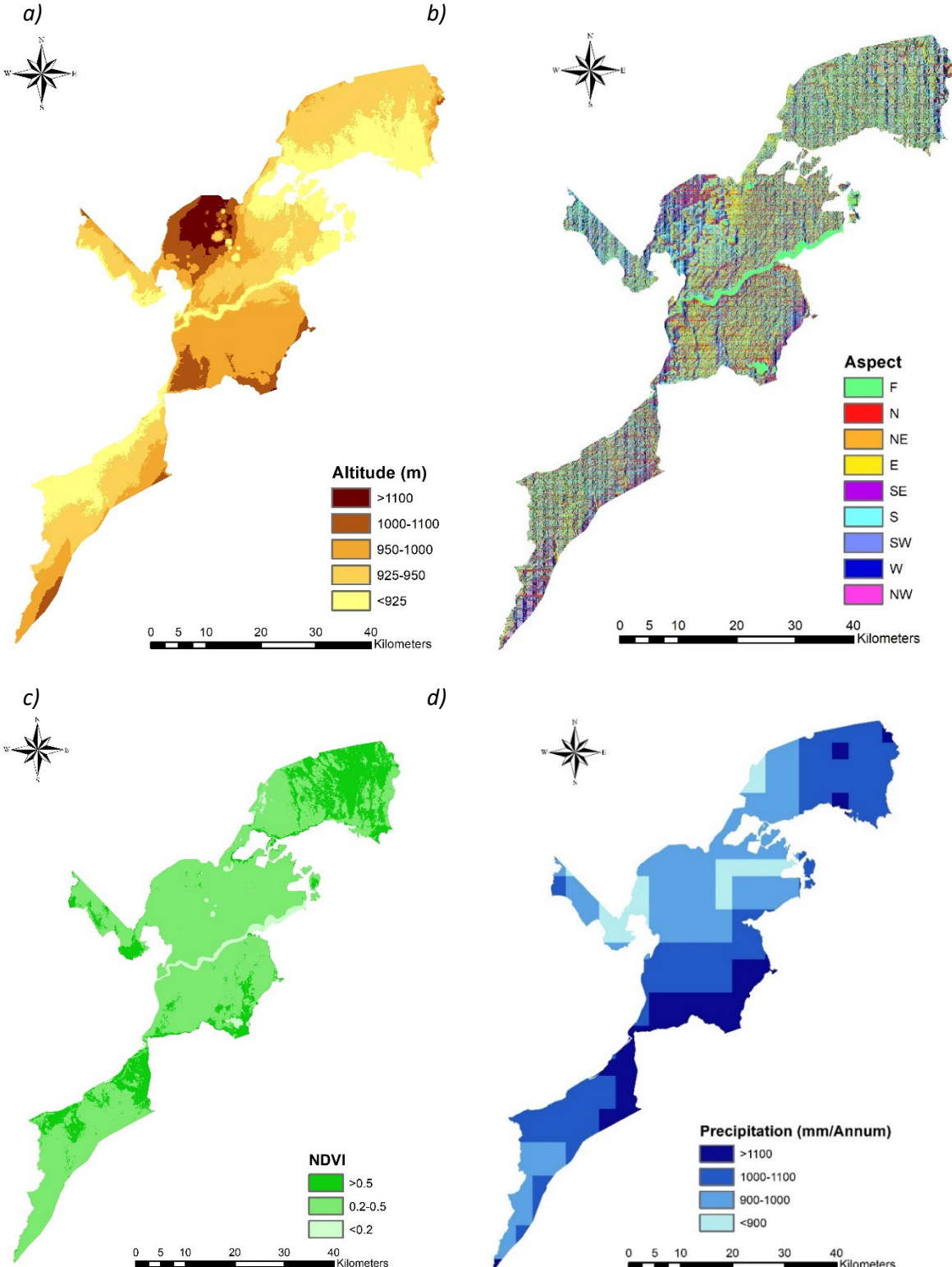


Figure 3: Average Monthly Distribution of Fires (2015-June 2021)

#### 4.4. Relationship between Wildfire Conditioning Factors and Wildfire Locations

The spatial relationships and significance levels of the relationships between the wildfire conditioning factors and the wildfire locations were derived from the WOE contrast values (C) and final weights ( $W_{final}$ ) respectively (Tables 1). The MODIS-derived C values showed relatively similar relationships for all the variables as compared to the VIIRS-derived C values. Generally, the VIIRS-derived  $W_{final}$  weights exhibited higher significance levels for similar variable categories as compared to the MODIS-derived  $W_{final}$  weights. The availability of more fire locations by VIIRS allowed for the accessing of more data to determine the spatial relationships between the wildfire conditioning factors and wildfires. As a result, more significant relationships were observed as compared to the MODIS-derived ones.



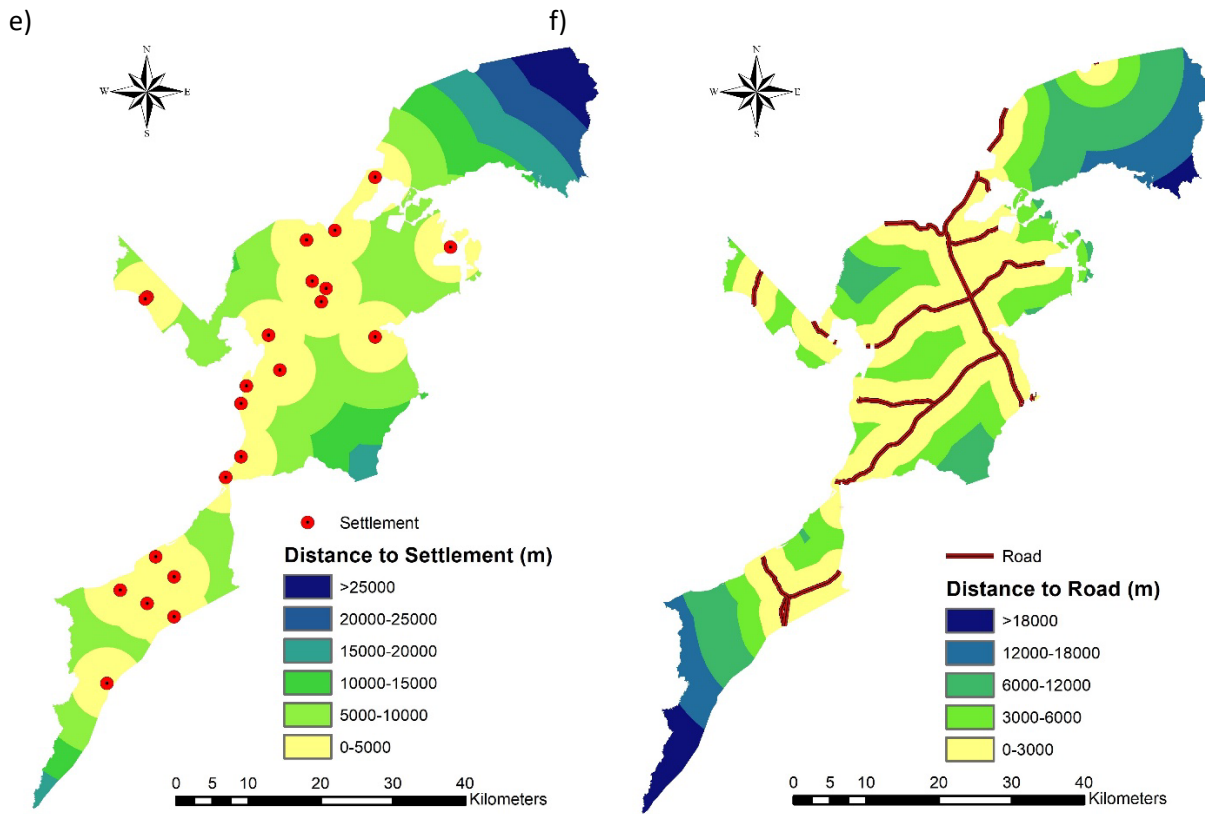


Figure 4: Wildfire Conditioning Factors: a) Altitude; b) Aspect; c) Vegetation (as measured by the NDVI); d) Precipitation; e) Distance from Settlement; f) Distance from Road; g) Distance from Lake; h) Distance from River

Table 1: WOE-derived Relationships between Wildfire Conditioning Factors and Wildfire Events

Variable	Class	Number of Pixels	% of Pixels	MODIS Fire Events	% of MODIS Fire Events	VIIRS Fire Events	% of VIIRS Fire Events	C (MODIS)	C (VIIRS)	$W_{final}$ (MODIS)	$W_{final}$ (VIIRS)
Aspect	F	630229	32.32	110	29.41	350	31.53	-0.137	-0.036	-0.56	-0.16
	N	264046	13.54	47	12.57	159	14.32	-0.086	0.065	-0.26	0.21
	NE	61802	3.17	12	3.21	29	2.61	0.013	-0.199	0.02	-0.33
	E	245944	12.61	48	12.83	129	11.62	0.020	-0.093	0.06	-0.30
	SE	67348	3.45	13	3.48	36	3.24	0.007	-0.065	0.01	-0.11
	S	244367	12.53	48	12.83	149	13.42	0.027	0.079	0.08	0.25
	SW	65887	3.38	13	3.48	47	4.23	0.029	0.234	0.05	0.41
	W	287401	14.74	69	18.45	153	13.78	0.269	-0.078	0.86	-0.27
	NW	82731	4.24	14	3.74	58	5.23	-0.131	0.219	-0.23	0.43
Ve Altitude (m)	<925	514021	26.36	166	44.39	534	48.11	0.802	0.951	3.21	4.05
	925 – 950	716128	36.73	144	38.50	387	34.86	0.076	-0.081	0.32	-0.37
	950 – 1000	485859	24.92	45	12.03	118	10.63	-0.886	-1.026	-3.16	-4.09
	1000 – 1100	168419	8.64	15	4.01	60	5.41	-0.817	-0.504	-1.84	-1.33
	>1100	65328	3.35	4	1.07	11	0.99	-1.165	-1.242	-1.56	-1.96
ge	<0.2	58546	3.00	3	0.80	15	1.35	-1.342	-0.815	-1.63	-1.27

	0.2 - 0.5	1498700	76.87	340	90.91	1028	92.61	1.102	1.328	3.70	5.04	
	>0.5	392509	20.13	31	8.29	67	6.04	-1.026	-1.367	-3.29	-4.89	
Precipitation (mm/Annum)	<900	160216	8.22	38	10.16	129	11.62	0.234	0.384	0.58	1.02	
	900 – 1000	729114	37.40	161	43.05		466	41.98	0.235	1.02	0.89	
	1000 - 1100	770250	39.50	135	36.10		395	35.59	-0.145	0.192	-0.63	
	>1100	290175	14.88	40	10.70	120	10.81	-0.378	-0.167	-0.366	-1.16	
Distance from Settlement (Km)	0 – 5	808826	41.48	143	38.24	382	34.41	-0.136	-0.301	-0.59	-1.42	
	5- 10	633510	32.49	152	40.64	485	43.69	0.352	0.478	1.48	2.15	
	10 – 15	182846	9.38	43	11.50	165	14.86	0.227	0.523	0.60	1.48	
	15 – 20	151162	7.75	26	6.95	60	5.41	-0.118	-0.386	-0.28	-0.97	
	20 – 25	100076	5.13	4	1.07	12	1.08	-1.610	-1.600	-2.38	-2.97	
	>25	73335	3.76	6	1.60	6	0.54	-0.874	-1.973	-1.31	-2.96	
Distance from Road (Km)	0 – 3	852837	43.74	163	43.58	470	42.34	-0.006	-0.057	-0.03	-0.27	
	3 – 6	484501	24.85	98	26.20	306	27.57	0.071	0.141	0.27	0.58	
	6 – 12	369077	18.93	71	18.98	206	18.56	0.004	-0.024	0.01	-0.09	
	12 – 18	174356	8.94	21	5.61	73	6.58	-0.501	-0.333	-1.20	-0.90	
	>18	68984	3.54	21	5.61	55	4.95	0.484	0.352	0.83	0.63	
Distance from River (Km)	0 – 1.5	663439	34.03	122	32.62	365	32.88	-0.063	-0.051	-0.27	-0.23	
	1.5 – 3	421578	21.62	89	23.80	289	26.04	0.124	0.244	0.46	0.97	
	3 – 6	314362	16.12	70	18.72	198	17.84	0.181	0.122	0.60	0.43	
	6 – 9	303591	15.57	57	15.24	147	13.24	-0.025	-0.189	-0.08	-0.65	
	>9	246785	12.66	36	9.63	111	10.00	-0.308	-0.266	-0.88	-0.84	
Distance from Lake (Km)	0 – 3	725383	37.20	53	14.17	170	15.32	-1.278	-1.187	-5.02	-5.32	
	3 – 6	565196	28.99	150	40.11	496	44.68	0.495	0.683	2.03	2.99	
	6 – 9	307073	15.75	92	24.60	237	21.35	0.557	0.373	1.86	1.31	
	9 – 15	270436	13.87	56	14.97	139	12.52	0.089	-0.118	0.28	-0.39	
	>15	81667	4.19	23	6.15	68	6.13	0.405	0.401	0.74	0.78	

Generally, an increase in altitude was found to be inversely related to the occurrence of fires. This can be attributed to the fact that wildfires at higher altitudes are less severe in the light of the increased moisture resulting from higher rainfall. Thus, fires tend to be prevalent at lower altitudes (Ganteaume *et al.*, 2013). As indicated by the  $W_{final}$  values, the correlation between aspect and fire incidents was found to be weak. Aspect determines the amount of solar energy received in an area (Pourghasemi, 2015) which depends on the latitude of an area or its location with respect to the equator and the season in which it finds itself the time of year and whether it is in the Northern or Southern Hemisphere. The study area provided a unique scenario by virtue of its being crossed by the equator, with portions in both the Northern and Southern Hemisphere. Thus, due to proximity of the study area to the equator, weak correlations were observed between aspect and fire occurrence.

Locations with NDVI values ranging between 0.2 - 0.5 experienced the highest incidence of fires, with 90.9% and 92.6% being MODIS and VIIRS fires respectively. Indeed, these same locations were strongly associated with the occurrence of fire. This is because low NDVI values point to water stress in vegetation, thereby implying high flammability (Bengtsson *et al.*, 2021; Verbesselt *et al.*, 2006). Increase in mean annual precipitation was negatively correlated with the occurrence of fires. Areas with low precipitation were associated with a high incidence of fires. As indicated by their negative  $W_{final}$  values

for both MODIS and VIIRS data, locations with the highest mean annual precipitation were least associated with the occurrence of fires. Precipitation contributes to the amount of moisture in the soil and vegetation. An increase in moisture is negatively correlated with the flammability of the combustible vegetation (Nhongo *et al.*, 2019).

Locations within five to fifteen kilometers of a settlement were associated with the occurrence of fires. Their positive  $W_{\text{final}}$  values could be attributed to this factor. These were characterized as grazing areas for livestock – a common agricultural activity within the study area. Pastoralists are known to set fire to the pastures at these locations to promote the growth of fresh grass (Uganda Wildlife Authority, 2012a). Distance from roads exhibited an extremely low significance in terms of its correlation with the occurrence of fire. Note that national roads and not smaller feeder and trail roads were considered in this study. In a previous study, Jaafari *et al.* (2017) indicated that local and feeder roads could cause human activities to exert a greater influence on fire ignition in that they more fully allow for a wider range of human mobility. This would lead to a stronger correlation between proximity to roads and the occurrence of fire.

$W_{\text{final}}$  values for both MODIS and VIIRS models indicated that locations close to water bodies are not associated with the occurrence of fire. Settlements further away from waterbodies exhibited positive  $W_{\text{final}}$  values, thereby indicating an association between this variable and fire incidents. Settlements near waterbodies, such as lakes and rivers, owe their location and development as settlements to fishing as the major economic activity. Activities of this nature are not associated with fire ignitions. Thus, such areas were negatively correlated with the occurrence of fires. However, Uganda Wildlife Authority (2012a) states that land further away from these fishing villages is used for other activities, including agriculture, the collection of firewood, and beekeeping, to cater for the ever-increasing populations in these communities which use fire for various purposes.

Vegetation (as measured by the NDVI), altitude, and distance from the lake were variables showing highly significant correlations with fire occurrences. This could be attributed to the existence of vast grasslands that provide the fuel for fires, the physiographic influence of altitude, as well as the socio-economic activities related to fishing villages. Aspect, precipitation, distance from a settlement, distance from a road, and distance from the river were variables showing extremely weak or insignificant correlations with the occurrence of fire.

#### **4.5. Wildfire Susceptibility Index Maps, Validation and Variable Importance**

The generated index maps, using natural breaks (Jenks), were classified into five classes of susceptibility, ranging from Very Low to Very High (Ghorbanzadeh *et al.*, 2019; Hong *et al.*, 2019). The success and prediction rates for all MODIS and VIIRS index maps are presented in Tables 2 and 3.

Table 2: MODIS AUC Success and Prediction Rates

Excluded Variable	AUC Success Rate (%)	AUC Prediction Rate (%)
None	69.9	66.1
Altitude	68.6	65.1
Aspect	69.8	66.4
Vegetation (as measured by the NDVI)	68.9	64.1
Precipitation	69.6	64.6
Distance from Settlement	69.7	65.8
Distance from Road	69.8	66.0
Distance from Lake	65.4	64.2
Distance from River	69.7	66.3

Table 3: VIIRS AUC Success and Prediction Rates

Excluded Variable	AUC Success Rate (%)	AUC Prediction Rate (%)
None	70.3	68.2
Altitude	69.9	67.3
Aspect	70.3	68.3
Vegetation (as measured by the NDVI)	68.3	67.3
Precipitation	70.0	67.7
Distance from Settlement	69.7	67.7
Distance from Road	70.2	68.3
Distance from Lake	66.8	64.9
Distance from River	69.9	68.1

Since two independent datasets (training and validation) were used for validation, two performance metrics were derived, namely, the success rate for the training data and the prediction rate for the validation data. From the ROC assessment, AUC values indicated that the performance of the VIIRS-derived model is slightly better than that for the MODIS-derived model. This was expected owing to the higher spatial resolution of the VIIRS-derived model. With all the variables included, a 69.9% success rate and a 66.1% prediction rate were achieved for the MODIS-derived model. These results indicate a model that performs moderately well (Gralewicz *et al.*, 2011). On the other hand, the VIIRS-derived model achieved a success rate of 70.3% and a prediction rate of 68.2%, thereby indicating a good model performance.

The performance of the MODIS-derived and VIIRS-derived models with all variables included, was at its best. As such, it was used for the generation of the wildfire susceptibility maps for both MODIS and VIIRS which are shown in Figure 5. Except for the northern end of the study area, most of the MODIS and VIIRS fires occurred within the regions classified with susceptibility levels of high and very high. This is consistent with the assumption about the application of the WOE model that future fire events are more likely to occur in areas with conditions like those that contributed to past events (Jaafari *et al.*, 2017). From the results, 18 - 19% of the study area is extremely susceptible to wildfires. This implies that 376 Km<sup>2</sup> of the 1,978 Km<sup>2</sup> of the study area are at a very high level of risk for wildfires. A further 20% (396 Km<sup>2</sup>) of the study area proved to be susceptible to fire, albeit at a reduced risk level. On the other hand, 42% of the study area, accounting for 831 Km<sup>2</sup>, was not susceptible to wildfires.

a)

b)

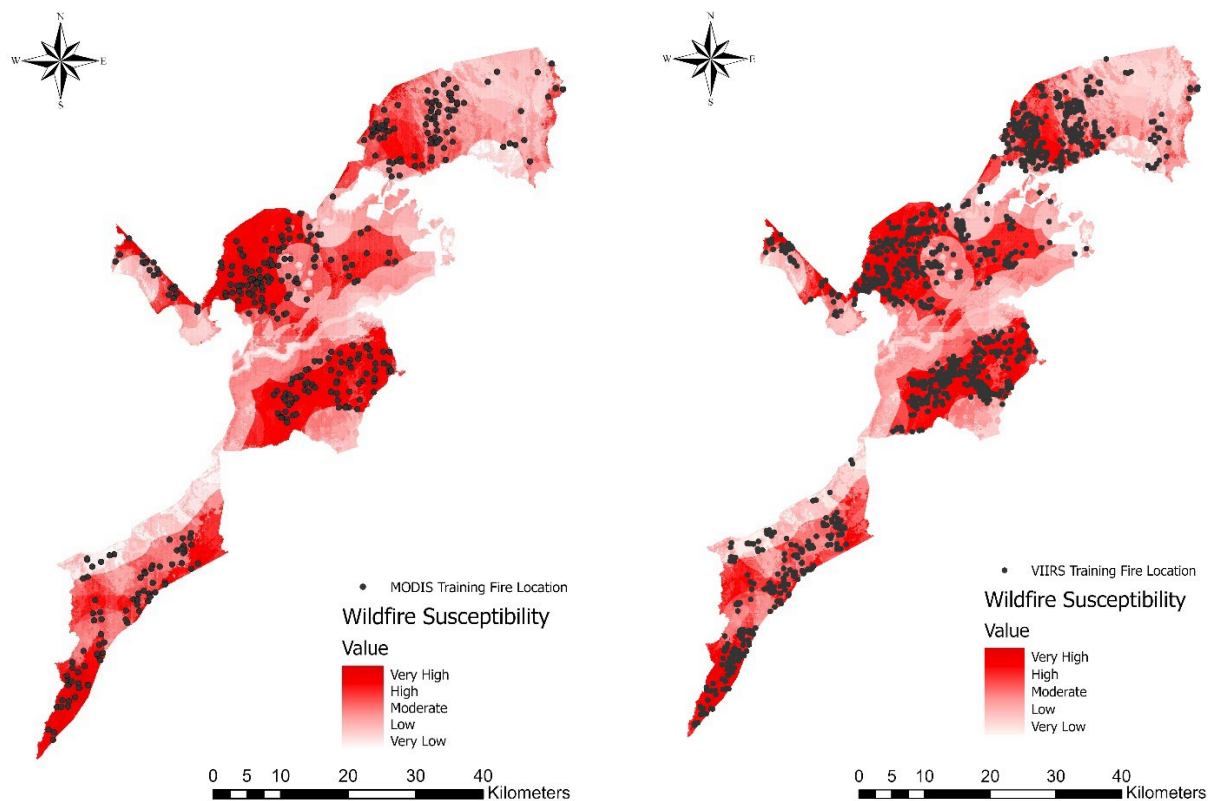


Figure 5: Wildfire Susceptibility: a) MODIS-derived model, b) VIIRS-derived model

## 5. Conclusion and Recommendations

The occurrence of fires within the study area is largely influenced by the season of the year, with most fires experienced during the dry season. This study provided information on when to apply fire prevention practices, such as prescribed burning and the provision of sensitized information against practices that could lead to wildfires. Furthermore, the MODIS and VIIRS datasets enabled the study of the distribution of fires from a spatio-temporal perspective. Additionally, despite the larger number of wildfires detected by VIIRS, both sensors identified similar wildfire susceptibility regions. The spatial distribution of fires within the study area not only underscores previous observations, but also indicates which places to prioritize while implementing wildfire management practices. Additionally, NDVI, that measures vegetation; altitude; and proximity to lakes proved to be the most influential wildfire conditioning factors in determining the occurrence of wildfires.

The wildfire susceptibility results enabled a narrowing-down of portions of the study area that were prone to the occurrence of wildfires. Given that the study area covers a large area (1,978 Km<sup>2</sup>), it was necessary to determine those portions on which to focus the limited fire management resources. Indeed, the wildfire susceptibility analysis indicated that areas with very high and high levels of susceptibility occupy 19% and 20% of the study area respectively. Therefore, the limited fire prevention and wildfire



suppression resources should be focused on areas with their priorities set according to the level of susceptibility since this is an indication of the likelihood that a fire would occur.

As recommendations, the study can be upscaled and used to develop early warning systems at the onset of the wildfire season. This can also be extended and applied to other landscapes with similar fire hazard issues. Future studies should also explore the inclusion of other factors that are documented to cause fires in the study area such as poaching. In the case of wildfire management, locations in the study area with high levels of susceptibility to fire should be prioritized. Owing to the dynamic nature of wildfire conditioning factors, the results pertaining to areas that are susceptible to wildfires are subject to change over time. This calls for the undertaking of similar studies periodically to better capture the current conditions.

## **6. Acknowledgment**

This paper is based on a study, the findings of which were presented at the Annual Geomatics Research Conference (AGRC) 2021 held at Makerere University, Kampala on the 8 October 2021.

## **7. References**

- Adab, H., Kanniah, K. D., & Solaimani, K. (2015). Modelling static fire hazards in a semi-arid region using frequency analysis. *International Journal of Wildland Fire*, 24, 763–777. <https://doi.org/10.1071/WF13113>
- Bengtsson, Z., Torres-pérez, J. L., & Mccullum, A. J. (2021). Satellites and Sensors for Vegetation-based Wildfire Applications (Post-Fire). National Aeronautics and Space Administration (NASA).
- CARE-Uganda. (2007). Conflict-sensitive Conservation: Field report from Queen Elizabeth National Conflict-sensitive Conservation Field.
- Chuvieco, E., & Congalton, R. G. (1989). Application of Remote Sensing and Geographic Information Systems to Forest Fire Hazard Mapping. *Remote Sensing of the Environment*, 159, 147–159. [https://doi.org/10.1016/0034-4257\(89\)90023-0](https://doi.org/10.1016/0034-4257(89)90023-0)
- De Meo, T., Barnett, J., & Small, E. (2010). USFS Trip Report - Fire Management and Planning in the Greater Virunga Landscape.
- Food and Agriculture Organisation of the United Nations. (2006). Global Forest Resources Assessment 2005 - Report on Fires in Sub-Saharan Africa Region (9; Fire Management).
- Ganteaume, A., Camia, A., Jappiot, M., San-Miguel-Ayanz, J., Long-Fournel, M., & Lampin, C. (2013). A review of the main driving factors of forest fire ignition over Europe. *Environmental Management*, 51(3), 651–662. <https://doi.org/10.1007/s00267-012-9961-z>
- Ghorbanzadeh, O., Kamran, K. V., Blaschke, T., Aryal, J., Naboureh, A., Einali, J., & Bian, J. (2019). Spatial Prediction of Wildfire Susceptibility using Field Survey GPS Data and Machine Learning Approaches. *Fire*, 2(43), 1–23. <https://doi.org/10.3390/fire2030043>
- Global Fire Monitoring Center. (2004). Wildland Fire Management Handbook for Sub-Saharan Africa (J. G. Goldammer & C. de Ronde, Eds.). Global Fire Monitoring Center.
- Gralewicz, N. J., Trisalyn, A., & Nelson, M. (2011). Factors influencing national scale wildfire susceptibility in Canada. *Forest Ecology and Management*, 265, 20–29. <https://doi.org/10.1016/j.foreco.2011.10.031>

- Hong, H., Jaafari, A., & Zenner, E. K. (2019). Predicting spatial patterns of wildfire susceptibility in the Huichang County, China: an integrated model for the analysis of landscape indicators. *Ecological Indicators*, 101(January), 878–891. <https://doi.org/10.1016/j.ecolind.2019.01.056>
- Hong, H., Tsangaratos, P., Ilija, I., Liu, J., Zhu, A., & Chen, W. (2018). Application of fuzzy weight of evidence and data mining techniques in the construction of a flood susceptibility map of Poyang County, China. *Science of the Total Environment*, 625, 575–588. <https://doi.org/10.1016/j.scitotenv.2017.12.256>
- Jaafari, A., Gholami, D. M., & Zenner, E. K. (2017). A Bayesian modelling of wildfire probability in the Zagros Mountains, Iran. *Ecological Informatics*, 39(2016), 32–44. <https://doi.org/10.1016/j.ecoinf.2017.03.003>
- Jaafari, A., Mafi-gholami, D., Pham, B. T., & Bui, D. T. (2019). Wildfire Probability Mapping: Bivariate vs Multivariate Statistics. *Remote Sensing*, 11(618), 1–18. <https://doi.org/10.3390/rs11060618>
- Jaafari, A., Zenner, E. K., & Pham, B. T. (2018). Wildfire spatial pattern analysis in the Zagros Mountains, Iran: a comparative study of decision tree-based classifiers. *Ecological Informatics*, 43, 200–211. <https://doi.org/10.1016/j.ecoinf.2017.12.006>
- Jahdi, R., Salis, M., Darvishsefat, A. A., Alcasena, F., Mostafavi, M. A., Etemad, V., Lozano, O. M., & Spano, D. (2016). Evaluating fire modelling systems in recent wildfires of the Golestan National Park, Iran. *Forestry*, 89(2), 136–149. <https://doi.org/10.1093/forestry/cpv045>
- Jones, M. W., Abatzoglou, J. T., Veraverbeke, S., Andela, N., Lasslop, G., Forkel, M., Smith, A. J. P., Burton, C., Betts, R. A., van der Werf, G. R., Sitch, S., Canadell, J. G., Santín, C., Kolden, C., Doerr, S. H., & Le Quéré, C. (2022). Global and Regional Trends and Drivers of Fire under Climate Change. In *Reviews of Geophysics* (Vol. 60, Issue 3). John Wiley and Sons Inc. <https://doi.org/10.1029/2020RG000726>
- Kayijamahe, C. B., Rwanyiziri, G., Mugabowindekwe, M., & Tuyishimire, J. (2020). Integrating Remote Sensing and GIS to Model Forest Fire Risk in Virunga Massif, Central - Eastern Africa. *Rwanda Journal of Engineering, Science, Technology, and the Environment*, 3 (Special), 146–166. <https://doi.org/10.4314/rjeste.v3i1.10S>
- Kganyago, M., & Shikwambana, L. (2019). Assessing Spatio-temporal Variability of Wildfires and their Impact on Sub-Saharan Ecosystems and Air Quality using Multisource Remotely Sensed Data and Trend Analysis. *Sustainability*, 11(6811). <https://doi.org/10.3390/su11236811>
- Lee, S., Kim, Y., & Oh, H. (2012). Application of a weights-of-evidence method and GIS to regional groundwater productivity potential mapping. *Journal of Environmental Management*, 96(1), 91–105. <https://doi.org/10.1016/j.jenvman.2011.09.016>
- Molaudzi, O. D., & Adelabu, S. A. (2018). Review of the Use of Remote Sensing for monitoring Wildfire Risk Conditions to support Fire Risk Assessment in Protected Areas. *South African Journal of Geomatics*, 7(3), 222–242. <https://doi.org/10.4314/sajg.v7i3.2>
- Nami, M. H., Jaafari, A., Fallah, M., & Nabiuni, S. (2018). Spatial prediction of wildfire probability in the Hyrcanian ecoregion using the evidential belief function model and GIS. *International Journal of Environmental Science and Technology*, 15(2), 373–384. <https://doi.org/10.1007/s13762-017-1371-6>
- Nhongo, E. J. S., Fontana, D. C., Guasselli, L. A., & Bremm, C. (2019). Probabilistic modelling of wildfire occurrence based on logistic regression, Niassa Reserve, Mozambique. *Geomatics, Natural Hazards, and Risk*, 10(1), 1772–1792. <https://doi.org/10.1080/19475705.2019.1615559>
- Ozdemir, A., & Altural, T. (2013). Journal of Asian Earth Sciences: a comparative study of frequency ratio, weights of evidence and logistic regression methods for landslide susceptibility mapping: Sultan Mountains, SW Turkey. *Journal of Asian Earth Sciences*, 64, 180–197. <https://doi.org/10.1016/j.jseaes.2012.12.014>

- Plumptre, A. J., Kirunda, B., Mugabe, H., Stabach, J., Driciru, M., Ayebare, S., Nangendo, G., & Laporte, N. (2010). The Impact of Fire and Large Mammals on the Ecology of Queen Elizabeth National Park.
- Pourghasemi, H. R. (2015). GIS-based forest fire susceptibility mapping in Iran: a comparison between evidential belief function and binary logistic regression models. *Scandinavian Journal of Forest Research*, May, 37–41. <https://doi.org/10.1080/02827581.2015.1052750>
- Pourtaghi, Z. S., Pourghasemi, H. R., Aretano, R., & Semeraro, T. (2016). Investigation of general indicators influencing forest fires and its susceptibility modeling using different data mining techniques. *Ecological Indicators*, 64, 72–84. <https://doi.org/10.1016/j.ecolind.2015.12.030>
- Sánchez, Y., Martínez-Graña, A., Santos Francés, F., & Mateos Picado, M. (2018). Mapping wildfire ignition probability using Sentinel 2 and LiDAR (Jerte Valley, Cáceres, Spain). *Sensors (Switzerland)*, 18(3), 1–18. <https://doi.org/10.3390/s18030826>
- Schroeder, W., Oliva, P., Giglio, L., & Csiszar, I. A. (2014). Remote Sensing of Environment: The New VIIRS 375 m active fire detection data product: algorithm description and initial assessment. *Remote Sensing of the Environment*, 143, 85–96. <https://doi.org/10.1016/j.rse.2013.12.008>
- Uganda Wildlife Authority. (2012a). Queen Elizabeth National Park, Kyambura Wildlife Reserve and Kigezi Wildlife Reserve General Management Plan (2011-2021).
- Uganda Wildlife Authority. (2012b). Queen Elizabeth National Park, Kyambura Wildlife Reserve and Kigezi Wildlife Reserve General Management Plan (2011-2021).
- Verbesselt, J., Somers, B., Van Aardt, J., Jonckheere, I., & Coppin, P. (2006). Monitoring herbaceous biomass and water content with Spot vegetation time-series to improve fire risk assessment in savanna ecosystems. *Remote Sensing of the Environment*, 101(3), 399–414. <https://doi.org/10.1016/j.rse.2006.01.005>
- Wimberly, M. C., Wanyama, D., Doughty, R., Peiro, H., & Crowell, S. (2024). Increasing Fire Activity in African Tropical Forests is associated with Deforestation and Climate Change. *Geophysical Research Letters*, 51(9). <https://doi.org/10.1029/2023GL106240>
- Xue, J., Li, K., Li, H., Wang, Y., Guo, X., Zhang, H., Zhao, J., & Chen, H. (2024). A novel data source for human-caused wildfires in China: extracting information from judgment documents. *Geomatics, Natural Hazards, and Risk*, 15(1). <https://doi.org/10.1080/19475705.2024.2361132>